Inorganic Chemistry

Article

pubs.acs.org/IC

Magnetic and Spectroscopic Investigation of Thermally and Optically Driven Valence Tautomerism in Thioether-Bridged Dinuclear Cobalt–Dioxolene Complexes

Giordano Poneti,*[,†,‡] Matteo Mannini,[†] Brunetto Cortigiani,[†] Lorenzo Poggini,[†] Lorenzo Sorace,[†] Edwige Otero,[§] Philippe Sainctavit,[∥] Roberta Sessoli,[†] and Andrea Dei[†]

[†]Laboratory of Molecular Magnetism (LaMM), Dipartimento di Chimica 'Ugo Schiff', Università degli Studi di Firenze & INSTM RU of Firenze, via della Lastruccia 3-13, 50019 Sesto Fiorentino, Italy

[‡]Dipartimento di Scienze e Tecnologie Applicate, Università "Guglielmo Marconi", Via Plinio 44, 00193 Roma, Italy

[§]Synchrotron SOLEIL, 91192 Gif-Sur-Yvette, France

[∥]Institut de Minéralogie et de Physique des Milieux Condensés, UMR 7590, CNRS, UPMC, IRD, 4 place Jussieu, 75005 Paris Cedex 5, France

Supporting Information

ABSTRACT: A series of dinuclear cobalt complexes of general formula $[Co(Me_ntpa)(diox\text{-}S\text{-}diox)Co(Me_ntpa)](PF_6)_2\cdot MeOH$ (n = 0, 2, 3) was prepared through the synthesis of the bis-bidentate ligand 6,6′-((1,4-phenylenebis(methylene))bis(sulfanediyl))bis(3,5-di-*tert*-butyl-benzene-1,2-diol) (diox-*S*-diox). The ancillary ligands Me_ntpa are obtained by the tripodal tris(2-pyridylmethyl)amine (tpa) ligand through successive introduction of methyl groups into the 6 position of the pyridine moieties. As expected, the steric hindrance induced by this substitution modulates the redox properties of the metal acceptor, determining the charge distribution of the metal–dioxolene adduct at room temperature. Magnetic measurements and X-ray photoelectron and X-ray absorption spectroscopies indicate that the charge distributions low-spin-Co^{III}–catecholate and high-spin-Co^{II}–semiquinonate characterize the complexes formed by the tpa and Me_3tpa tetradentate ligands, respectively. The complex formed by the Me_2tpa ligand undergoes a thermal- and light-induced interconversion of the two states, in agreement with the existence of a valence tautomeric equilibrium. All complexes were stable and behaved reproducibly under X-ray irradiation. This work points out a fast and simple chemical approach to structurally and electronically modify the catechol ring while leaving its coordination capabilities unaffected. These findings afford a robust chemical method to prepare sulfur-functionalized dioxolene ligands as new molecular bricks for chemical functionalization of noble metal surfaces with this class of molecular switches.

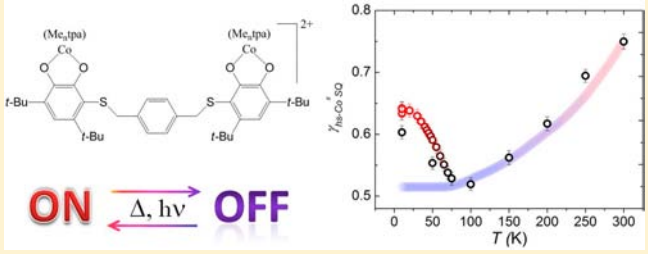

INTRODUCTION

Molecular systems displaying tunable physical response (switchability) are considered key active materials for fabrication of next-generation sensors, data storage, and information-processing devices.[1,2] Molecular-based switchable paramagnetic units, in particular, are intensively investigated within the framework of molecular spintronics for their intrinsic possibility of existing in different electronic configurations, each of them featuring its own physical properties.[3] In this context molecules characterized by electronic lability, like mixed-valence,[4] spin crossover (SCO),[1,3] and redox isomeric (also known as valence tautomeric, VT)[5] complexes, are particularly appealing.

Cobalt complexes with dioxolene ligands belong to the latter class of switchable molecules. They behave as class II mixed-valence materials,[6] showing a small but finite degree of electronic delocalization between the Co ion and the organic ligand. This allows the definition of two possible electronic states in the molecular framework: the closed-shell *ls*-Co^{III}(Cat) one and its paramagnetic redox isomer, *hs*-Co^{II}(SQ), where Cat and SQ stand for catecholate and semiquinonate forms of the dioxolene ligand, respectively.[7] Low temperatures stabilize the former state for enthalpic reasons, since it features shorter coordination lengths and zero-spin degeneracy. Upon heating, a reversible intramolecular electron transfer takes place from the dioxolene ligand to the Co ion, leading to the switch of the spin state of the latter. This transformation is driven by the entropic gain arising from the higher density of vibrational and spin states in the *hs*-Co^{II}(SQ) redox isomer.[8]

Variation of thermodynamic parameters, such as temperature,[4,9−13] pressure,[14−16] and magnetic field,[17] allows one to

Received: May 13, 2013
Published: October 4, 2013

   dx.doi.org/10.1021/ic4011949 | *Inorg. Chem.* 2013, 52, 11798−11805

control the charge distribution of the system by tuning the energy difference between its different electronic states. This transition can also be achieved optically at cryogenic temperatures,[7,18] where irradiation on the ligand to metal charge transfer bands populates the metastable *hs*-Co^{II}(SQ) electronic state. Its low electronic and vibrational coupling with the ground *ls*-Co^{III}(Cat) state gives rise to an activation barrier to the relaxation process and thus to a temperature-dependent decay rate. In both SCO[19] and VT materials[20] the thermal and optical bistabilities follow two different behaviors. Temperature-induced transitions are strictly related to environmental effects (like crystal packing features: molecular volume in the lattice, nature of the counteranion, sample crystallinity, and intermolecular interactions); on the contrary, the decay process of the photoinduced phase is less sensitive to the molecular surroundings, being ruled by single-molecule properties like variation of bond lengths taking place during the optically triggered transition.

In view of potential applications these findings are extremely promising, suggesting that bistable molecular materials may be used in nanosized devices. Several groups have investigated the effects of size reduction on the retention of thermally driven bistability using different approaches, ranging from preparation of nanoparticles,[21] thin films,[22] down to submonolayer coverages.[23,24] Moreover, it has been recently proposed, on the basis of DFT calculations, that the electric potential available in an STM experiment may be used to both read and change the electronic ground state of VT systems when isolated on conductive surfaces.[25] In this perspective, chemical functionalization of the redox-active cobalt−dioxolene molecular core, along with preservation of its switchability features, represents a crucial step toward nanostructuration of these systems.

In this work we present the synthesis and multitechnique characterization of a family of dinuclear cobalt−dioxolene complexes chemically functionalized with a thioether bridge, a possible building block for development of switchable molecular nanostructures. We used the Michael addition of thiols to quinones to synthesize a new tetraoxolene ligand 6,6′-((1,4-phenylenebis(methylene))bis(sulfanediyl))bis(3,5-di-*tert*-butyl-benzene-1,2-diol) (diox-*S*-diox, from now on). Following a previously defined chemical strategy for control of the redox potential of the $Co(Me_ntpa)^{3+/2+}$ couples[26] (Me_ntpa = ligand obtained by introduction of *n*-methyl groups in the 6- position of the different pyridine moieties of the tris(2-pyridylmethyl)-amine ligand, Figure 1), we prepared three different derivatives with general formula $[Co(Me_ntpa)diox\text{-}S\text{-}dioxCo(Me_ntpa)](PF_6)_2\cdot MeOH$ (**1** for n = 0, **2** for n = 2, and **3** for n = 3). Finally, magnetometry, X-ray photoelectron spectroscopy (XPS) and X-ray absorption spectroscopy (XAS) have been used to study their electronic structures.

EXPERIMENTAL SECTION

General Remarks. All commercially available chemicals and solvents were of reagent grade and used as received. Me_ntpa ligands were synthesized according to a previously reported synthetic procedure.[26]

Synthesis of diox-*S*-diox. To a 30 mL hexane solution of 3,5-di-*tert*-butyl-quinone (0.66 mmol, 145 mg) under magnetic stirring, 1,4-benzen-dimethanthiol (0.3 mmol, 51 mg) was added. After a few minutes the solution began to turn colorless, and in 30 min a white precipitate appeared. The white powder was filtered, recrystallized from hexane, and dried in vacuum. Yield: 81%. ^{1}H NMR (400 MHz; $CDCl_3$): 7.19 (s, 4H); 7.10 (s, 2H); 6.94 (s, 2H); 5.59 (s, 2H); 3.81 (s, 4H); 1.52 (s, 18H); 1.42 (s, 18H). Anal. Found: C, 70.51; H, 8.02. Calcd for $C_{36}H_{50}O_4S_2$: C, 70.78; H, 8.25.

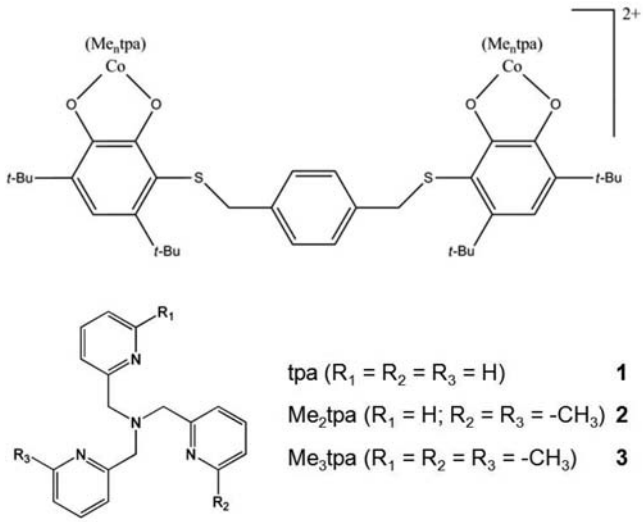

Figure 1. Schematic representation of the molecular core of the family of complexes **1** (n = 0), **2** (n = 2), **3** (n = 3), and the corresponding ancillary Me_ntpa ligands.

Synthesis of the $Co_2(Me_ntpa)_2$diox-*S*-diox$(PF_6)_2\cdot$MeOH Complexes (1−3). Synthesis of **1**−**3** was performed following the procedure developed for unfunctionalized 3,5-di-*tert*-butyl derivatives, previously reported.[26] To a warm methanolic solution (30 mL) of $CoCl_2\cdot 6H_2O$ (0.2 mmol, 47.6 mg) and Me_ntpa (0.22 mmol, n = 0 for **1**, n = 2 for **2**, and n = 3 for **3**) under inert atmosphere, a methanolic solution of triethylamine tetra-deprotonated diox-*S*-diox ligand (0.1 mmol, 61 mg) was added. After 10 min of magnetic stirring the solution was exposed to air to help with the oxidation with dioxygen, and then the compounds were precipitated adding a water solution of KPF_6. Solids were then recrystallized from methanol, yielding analytically pure samples. **1**: yield 54%. Anal. Found: Co, 7.16; C, 53.36; H, 5.40; N, 7.02. Calcd for $Co_2C_{74}H_{90}N_8O_6S_2P_2F_{12}$: Co, 7.10; C, 53.56; H, 5.47; N, 6.75. **2**: yield 63%. Anal. Found: Co, 6.74; C, 53.06; H, 4.69; N, 6.65. Calcd for $Co_2C_{78}H_{98}N_8O_6S_2P_2F_{12}$: Co, 6.87; C, 54.61; H, 5.76; N, 6.53. **3**: yield 61%. Anal. Found: Co, 6.79; C, 55.44; H, 6.42; N, 6.55. Calcd for $Co_2C_{80}H_{102}N_8O_6S_2P_2F_{12}$: Co, 6.76; C, 55.11; H, 5.90; N, 6.43. Electronic absorption spectra and IR spectra of complexes **1**−**3** are reported as Figures S1 and S2, respectively.

Physical Measurements and Instrumentation. Elemental analysis was carried out on a Carlo Erba EA1110 CHNS-O automatic analyzer. Determination of cobalt concentration was performed with a Varian 720-ES Inductively Coupled Plasma Atomic Emission Spectrometer (ICP-AES). ^{1}H NMR spectra in $CDCl_3$ solution were recorded at 298 K on a 400 MHz Bruker Avance III spectrometer. Chemical shifts are given in ppm downfield from TMS. UV−vis spectra of dichloromethane solutions were recorded on a Jasco V70 spectrophotometer using quartz cells with 1 cm optical path; powders data were acquired on the same instrument using an integrating sphere. IR spectra of Nujol dispersions were acquired on a Perkin-Elmer spectrumBX system. Thermogravimetric analyses of powder samples were performed using an EXSTAR Thermo Gravimetric Analyzer (TG/DTA) Seiko 6200.

Magnetic Susceptibility Measurements. Magnetic investigations were performed on powdered samples using a Quantum Design MPMS instrument equipped with a 5 T magnet. The temperature dependence of the magnetization (M) was followed from 1.8 to 300 K by applying a 10 kOe field (H) from 300 to 45 K and a 1 kOe field below 45 K to reduce magnetic saturation effects. Magnetic susceptibility per mole (χ_M) was then evaluated as $\chi_M = M_M/H$. Magnetic data were corrected for the sample holder contribution and for the sample diamagnetism using Pascal's constants. *hs*-Co^{II} molar

dx.doi.org/10.1021/ic4011949 | *Inorg. Chem.* 2013, 52, 11798−11805

fraction has been calculated from magnetometric data according to Equation S1, Supporting Information.

Photomagnetic Measurements. Photomagnetic characterization was obtained by mixing approximately 0.5 mg of microcrystalline powder with KBr powder pressed into a pellet to facilitate light penetration. The actual Co content was then evaluated by scaling the magnetic moment of the pellet on that of a crystalline heavier sample. Irradiation experiments have been performed at 904 nm coupling the specific continuous wave (CW) laser diode with an optical fiber inserted in the sample space through a hollow sample rod and collimated on the sample by means of an aspheric lens, yielding a radiant power on the sample of about 5 mW cm^{-2}. The excitation wavelength has been selected to match the LMCT band of the electronic spectrum of the *ls*-Co^{III}(Cat) chromophore and minimize its spectral overlap with the MLCT band of the *hs*-Co^{II}(SQ) one, reported in Figure S1, Supporting Information, in accordance with previous reports about Co−diox photoswitchable systems.[27,28] Magnetic moments were corrected for the diamagnetic contribution of the KBr and the sample holder, independently measured in the same range of field and temperature. T_{LIESST} measurement consisted in monitoring the temperature featuring a minimum in the $d(\chi_M T)/dT$ curve after reaching the photostationary limit, having switched the laser off at 10 K, and warming the sample at a rate of 0.3 K/min.[7,19,29]

XPS. XPS experiments were performed using nonmonochromatized Al Kα radiation in a ultra-high-vacuum (UHV) apparatus consisting of one chamber with a base pressure in the low end of the 10^{-9} mbar range. The angle between the analyzer axis and the X-ray propagation vector from the X-ray source was 54.44°. XPS spectra were measured with a fixed pass energy of 44 eV. The binding energy (BE) scale was calibrated setting the F_{1s} photoemission peak of the PF_6^- ion, present in each complex, to 687.2 eV, according to earlier reports.[30] Samples have been measured in the solid state as powder pressed on top of carbon tape. Data analysis was performed with XPSPeak41 software using mixed Gaussian and Lorentzian line shapes, and the inelastic background in the spectra was subtracted by means of a Shirley function. The elemental composition of the samples was then evaluated using a semiempirical approach: the integrated intensity of each component not affected by spurious contribution was corrected for the photoionization cross-section of each element.[31]

X-ray Absorption Spectroscopy. XAS spectra have been acquired at the ID08 beamline of the European Synchrotron Radiation Facility (ESRF) in Grenoble, France. X-ray absorption spectra have been measured on a drop-cast sample of **2** from dichloromethane, inserted in a special holder designed to allow sample irradiation with both an X-ray beam and a CW 904 nm laser beam. The photon flux per second of the 904 nm laser was 10 mW/cm^2 on the sample. The holder was inserted in a cryostat working in the 8−320 K temperature range, and the X-ray photon flux onto the sample was reduced in order to ensure no radiation damage. The reduction was obtained by inserting horizontal and vertical baffles downstream the Apple II ID08 undulator and selecting 10 μm × 10 μm for the entrance and exits slits of the Dragon monochromator.

RESULTS AND DISCUSSION

Synthesis. In order to prepare a thioether-functionalized catechol ligand, the best approach was found to be the addition of thiols to quinones. The reactivity of quinones toward thiols is indeed well known:[32] following a Michael addition mechanism, the nucleophilic thiol binds to the quinone ring, affording the catechol adduct in high yields and very short reaction times.[33] A similar procedure has been used to prepare quinone-based self-assembled monolayers on different surfaces using a click chemistry approach.[34,35]

The diox-*S*-diox bis-catechol ligand was prepared by slow addition of solid 1,4-benzen-dimethanthiol to a hexane solution of 3,5-di-*tert*-butyl-quinone in slight excess. After a few minutes, the green solution turned colorless and white powder precipitated. The diox-*S*-diox ligand was then obtained through recrystallization from hexane. 2D NOESY NMR cross-peak signals unambiguously pointed out addition of the thiol in the less sterically hindered 6 position of the quinone ring, with no detected signal of different regioisomeric adducts (see Figure S3, Supporting Information). Preparation of complexes **1**−**3** involved addition of a methanolic solution of tetra-deprotonated diox-*S*-$diox^{4-}$ to a warm methanolic solution of $Co(Me_ntpa)^{2+}$ (n = 0, 2, and 3 for complexes **1**, **2**, and **3**, respectively) under inert atmosphere, even if not always required. The corresponding neutral $[Co_2(Me_ntpa)_2$diox-*S*-diox] complexes underwent a doubly electron oxidation upon exposure to dioxygen and subsequently precipitated after addition of an aqueous solution of KPF_6. Recrystallization from methanol yielded analytically pure powders of **1**−**3** complexes. Despite the fact that attempts to obtain suitable crystals for X-ray diffraction studies failed, elemental analysis, spectroscopic investigations, and magnetic data unequivocally demonstrate the formation of the molecular structure sketched in Figure 1.

Magnetic Characterization. Temperature- and light-dependent magnetic measurements are a very powerful tool to follow the conversion between the diamagnetic *ls*-Co^{III}(Cat) and the paramagnetic *hs*-Co^{II}(SQ) isomers. Figure 2 reports the temperature dependence of the $\chi_M T$ product of complexes **1**, **2**, and **3**.

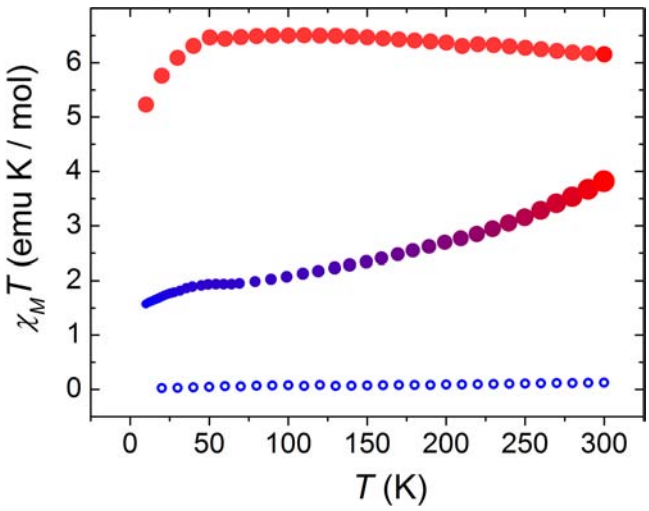

Figure 2. Temperature dependence of the $\chi_M T$ product of **1** (small blue empty circles), **2** (changing full circles), and **3** (large full red circles), measured applying a 1 kOe field in the 2−45 K range and a 10 kOe one up to 300 K.

1 shows a completely diamagnetic behavior in the 10−300 K range, its $\chi_M T$ varying from 0.02 emu K/mol at 10 K to 0.13 emu K/mol at 300 K, in line with the expected temperature-independent paramagnetism of the octahedrally coordinated *ls*-Co^{III} ion.[36] This clearly indicates a temperature-independent *ls*-Co^{III}(Cat) electronic distribution in the whole temperature interval investigated. On the contrary, the room-temperature $\chi_M T$ value of **3** (6.15 emu K/mol) is consistent with two noninteracting semiquinonate radical ligands (S = 1/2, g =2.0) and two *hs*-Co^{II} ions (S = 3/2 with significant orbital contribution) and is in the range expected for two *hs*-Co^{II}−SQ moieties (6.0−7.6 emu·K/mol).[37] The weak increase in $\chi_M T$ observed on lowering temperature, albeit surprising at first sight, has already been reported by some of us for a different

dx.doi.org/10.1021/ic4011949 | *Inorg. Chem.* 2013, 52, 11798−11805

dinuclear cobalt−-dioxolene system.[28] This can be attributed to variable population of the excited multiplets of the $^4T_{1g}$ ground state of Co^{II} centers, which is split due to the combined effect of low symmetry distortion and spin−orbit coupling.[37,38] As a whole, these data indicate a temperature-invariant *hs*-Co^{II}SQ charge distribution for both moieties of **3**.

The temperature dependence of the $\chi_M T$ product of **2** is completely different, varying from 3.82 emu K/mol at 300 K to 1.93 emu K/mol at 60 K, in accordance with a thermally driven valence tautomeric equilibrium. Deconvolution of the magnetic signal of **2** using **1** and **3** as reference compositional cases for the *ls*-Co^{III}(Cat) and *hs*-Co^{II}(SQ) charge distributions, respectively, allows one to estimate a *hs*-Co^{II}(SQ) molar fraction of 61% at 300 K.[39] Despite its dinuclear nature, no evidence of double-stepped entropy-driven conversion was found for **2**. This can be explained considering the lack of proper structural rigidity of the thioetheric bridge, which makes it unable to vibronically couple the two different Co−diox centers. Molecular-based multistability in Co VT molecular materials, reported for the first time by Preuss and co-workers for an amorphous film of a dinuclear cobalt−dioxolene complex,[40] was indeed recently shown to depend on the vibronic coupling between the two Co−diox moieties.[28] Below 60 K, the leveling of $\chi_M T$ of **2** to 1.57 emu K/mol is indicative of the presence of a *hs*-Co^{II}(SQ) remaining fraction at low temperature (29% of the overall Co content). This behavior, usually observed in spin cross-over complexes[41] and molecules undergoing redox isomerism,[20] is to be attributed to the negligible intermolecular cooperativity in the solid state, confirmed by the smooth profile of entropy-driven transition.

Photomagnetism. In line with previously characterized cobalt−dioxolene complexes undergoing temperature-induced VT behavior,[11] **2** behaves as a light-induced paramagnetic switch, showing the possibility to optically trigger the *ls*-Co^{III}(Cat) to *hs*-Co^{II}(SQ) conversion when irradiating on the LMCT band of the low-temperature chromophore. Figure S5, Supporting Information, reports the effect of the application of 904 nm laser light on sample **2**: its $\chi_M T$ value increases from 1.57 up to 1.99 emu·K/mol, corresponding to an 11% photoconversion of the *ls*-Co^{III}(Cat) content at 10 K. In order to characterize the relaxation dynamics of the photoinduced metastable *hs*-Co^{II}(SQ) molar fraction ($\gamma_{hs\text{-}Co(II)SQ}$) to the *ls*-$Co^{III}$(Cat) electronic ground state for **2**, the time-dependent decays of the photoinduced *hs*-Co^{II}(SQ) have been measured (Figure 3). Its relaxation times τ (defined as the time needed for the photoinduced phase to relax to a (1/e) fraction of its starting value) at different temperatures were thus extracted by a least-squares fitting of the curves. The model employed to fit the data was the exponential decay one: $\gamma_{hs}(t) = \gamma_{hs}(0)\exp[-(t/\tau)^{\beta}]$, where β is a parameter taking phenomenologically into account a distribution of relaxation times[42] (see Table S1, Supporting Information, for the set of best-fit parameters at different temperatures). The extracted relaxation times feature a nonlinear dependence on temperature: monitoring the $\ln(\tau)$ vs T^{-1} plot (inset of Figure 3), it is possible to distinguish a crossover between a low-temperature regime (10−20 K), where τ is temperature independent, and a higher temperature one (30−60 K), where a linear dependence of τ with T^{-1} is clearly observed. The fit of these points by an Arrhenius model for thermally activated relaxation ($\tau(T) = \tau(0)\exp(-\Delta/k_BT)$) resulted in a pre-exponential factor of 25(15) s and an activation barrier (Δ) of 221(16) cm^{-1}. This confirms that the mixing of the metastable and ground

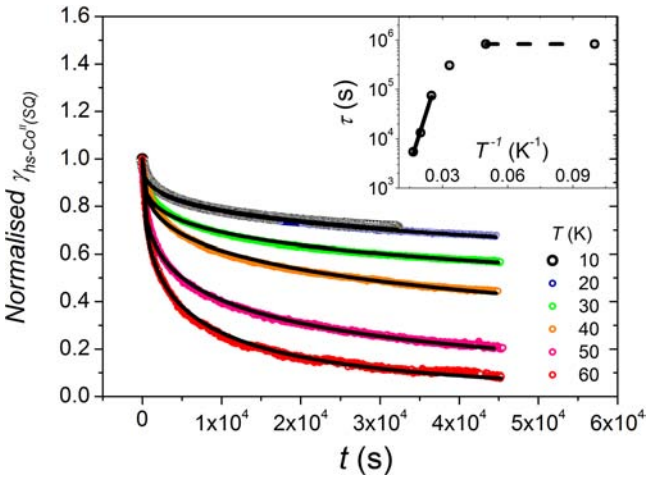

Figure 3. Isothermal time dependence of the photoinduced *hs*-Co^{II}(SQ) molar fraction of **2**, measured at different temperatures after photoexcitation at 10 K. Best-fitting lines have been calculated as described in the text. (Inset) Corresponding Arrhenius plot, with high-temperature (full) and low-temperature (dashed) best-fit lines (see text).

electronic states responsible for the decay takes place mainly though the Co−O stretching vibrational mode.[26,27] Linear fit of the low-temperature region (reported in Figure 3 as a dotted line) yielded 8.2(1) × 10^5 s as $\tau(0)$.

An estimate of the energy barrier to the thermally activated relaxation of the photoinduced phase can also be obtained by analyzing the thermal dependence of its metastable molar fraction $\gamma_{hs\text{-}Co(II)SQ}$ (Figure S6, Supporting Information). After switching off the excitation source at 10 K, the $\chi_M T$ value collapses on the nonirradiated one at 78 K. If carried out at a warming rate of 0.3 K min^{-1}, this process allows one to measure the T_{LIESST} parameter, i.e., the temperature where a minimum in the $d(\gamma_{hs\text{-}Co(II)SQ})/dT$ vs T plot occurs.[29,43] This parameter affords an easy way to compare the stability of the photoinduced state for different optically switchable materials. For **2**, the derived value of T_{LIESST} is 49 K, in agreement with literature data about photoswitchable cobalt−dioxolene complexes relying on the $[CoN_4$dioxolene$]^+$ molecular core, where N_4 stands for the four nitrogen-donor atoms of either one (tetradentate) or two (bidentate) ancillary ligands.[11,20,27,38,44]

X-ray Photoelectron Spectroscopy. XPS has been previously used as an atomically specific spectroscopic probe of oxidation and spin states in the analysis of electronic structures of molecular switchable materials, ranging from mixed-valence[45] to spin crossover[46] and coordination polymeric networks.[47−50] In dioxolene−metal coordination chemistry it has allowed to determine the charge distribution in different nickel−dioxolene adducts.[51] Moreover, its surface sensitivity can provide information about chemical and electronic structures of diluted samples like monolayers of molecules grafted to conductive surfaces. However, since the binding energy of a given orbital is dependent on both valence and spin configuration of the emitter, it is not always straightforward to address redox states when the spin state of the emitter can be switched as well.[52] By comparing the Co2p XPS spectra of **2** with those of the limiting charge configuration cases **1** and **3** it is possible to achieve a reference set to estimate the charge distribution of the interconverting system.

dx.doi.org/10.1021/ic4011949 | Inorg. Chem. 2013, 52, 11798−11805

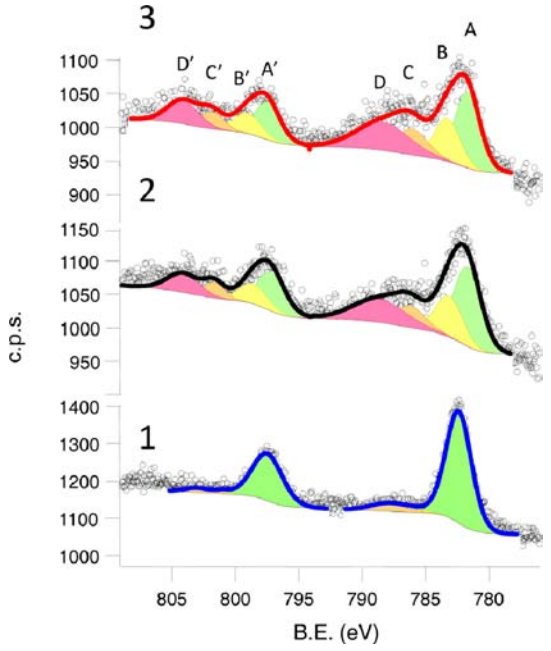

Figure 4. Co2p room-temperature XPS spectra of compounds **1**−**3** along with best-fit components, as reported in Table 1 (intensity is expressed in counts per second, cps).

The first step of our XPS analysis involved a semiquantitative determination of the elemental composition of **1**−**3** using Co2p (Figure 4), N1s, S2p, P2p, and F1s (Figure S7, Supporting Information) core levels. Carbon and oxygen contributions were discarded since they may be affected by spurious contaminations. This analysis confirms the theoretical stoichiometric composition of the complexes, which is expected to be the same for the three compounds with regard to the investigated elements (see Table 1). The experimental ratios between the most significant contributions (Co/N, Co/S, Co/P) agree as well with the theoretical ones.

Additional information can be extracted analyzing the line shape of the Co2p spectra of **1**−**3**. This region was fitted following a previously reported procedure for *ls*-Co^{III} and *hs*-Co^{II} complexes;[53,54] Table 1 and Figure 4 report the results of the fitting analysis. The $Co2p_{3/2}$ region has been reproduced with 3 or 4 components (A−D) along with the corresponding $Co2p_{1/2}$ spin−orbit (SO) coupled contributions (A′−D′) weighted by the expected 2:1 ratio. In agreement with literature reports, the SO shift depends on the Co redox state and is larger for the *hs*-Co^{II} ion than for the *ls*-Co^{III} one (15.8 eV for **3** and 15.1 eV for **1**). This indicates that complex **2**, whose room-temperature SO shift is 15.5 eV, is constituted mainly by *hs*-Co^{II} ions but indeed contains a relevant *ls*-Co^{III} molar fraction, in agreement with magnetometric, UV−vis (Figure S1, Supporting Information), and IR spectroscopic data (Figure S2, Supporting Information). Moreover, the Co2p spectrum of **1** can be reproduced by a main peak (A) centered at 782.4 eV, with only minor contributions at higher binding energies (B, C, plus the corresponding SO peaks), in line with the electronic ground state expected for an octahedrally coordinated *ls*-Co^{III} ion ($^1A_{1g}$).[55] Compounds **2** and **3**, on the contrary, display more complex spectral patterns due to the presence of shakeup components, typical of *hs*-Co^{II} systems in octahedral coordination environment and in line with previous reports about inorganic[56] and metallorganic[53] *ls*-Co^{III} and *hs*-Co^{II} compounds.

This approach points out that comparison of XPS spectra of structurally related VT complexes can be used as an in-house analytical tool to obtain information about their electronic charge distribution. A quantitative description of their temperature and light conversion features, however, requires higher sensitivity techniques, like synchrotron-based absorption spectroscopies.

X-ray Absorption Spectroscopy. The charge distribution of the bulk phase of **1**−**3** has been assessed using temperature- and light-dependent XAS. In the past, XAS was shown to be an unmatched tool for analysis of thermally and optically triggered transitions of bistable molecular materials, affording spectral analysis of the processes with atomic selectivity and sensitivity to investigate bulk and surface-confined molecular assemblies.[57] More specifically, it has been employed to study the electronic and structural features of switchable materials like polycyanometallates[58] and Fe^{II} complexes[59,60] as well as to investigate the effect of surface confinement on their bistability.[23,61] In the case of VT materials, it helped in clarifying the electronic states involved in the pressure-,[14] entropy-,[62,63] and light-driven conversions[64] and revealed X-ray light as an optical source of photoconversion, though the microscopic mechanism involved

Table 1. Results of XPS Spectral Fitting of 1−3, along with Semi-Quantitative Evaluation of Their Chemical Composition

	Co2p										
	components										
		A		B		C		D			
	%[a]	BE[b]	(%)	BE[b]	(%)	BE[b]	(%)	BE[b]	(%)	SO[c]	
1	**7.4**	782.4	(89.2)	786.0	(2.5)	788.0	(8.3)	n.a.	(n.a.)	15.1	
2	**7.6**	781.6	(42.1)	783.2	(21.5)	786.2	(12.5)	788.6	(23.9)	15.5	
3	**7.3**	781.7	(36.3)	783.3	(20.7)	786.0	(15.1)	788.4	(27.9)	15.8	
theor	7.7										
N1s			S2p			P2p			F1s		
%[a]	BE[b]	Co/N	%[a]	BE[b]	Co/S	%[a]	BE	Co/P	%	BE	
31.6	401.3	0.2	**6.5**	164.0	1.1	**7.2**	137.2	1.0	**47.2**	687.2	
30.6	401.0	0.3	**7.5**	164.4	1.0	**6.2**	137.2	1.2	**48.1**	687.2	
27.9	400.8	0.3	**7.1**	164.4	1.0	**7.8**	137.2	0.9	**49.9**	687.2	
30.8		0.3	7.7		1.0	7.7		1.0	**46.2**		

[a]Molar percentage of XPS-monitored elements. [b]Binding energies (BE) in eV. Component contributions are reported in brackets. [c]Spin−orbit splittings in eV.

dx.doi.org/10.1021/ic4011949 | *Inorg. Chem.* 2013, 52, 11798−11805

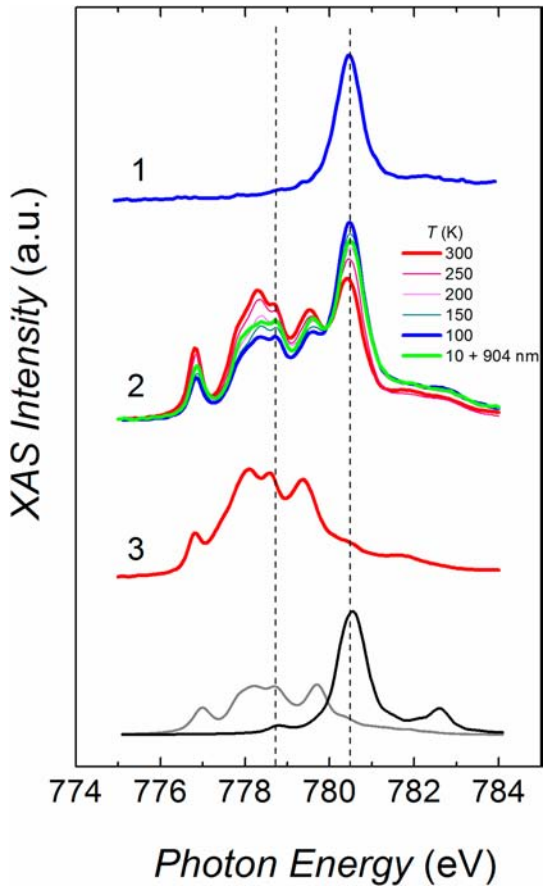

Figure 5. Co L_3 edge X-ray absorption spectra of **1**−**3** along with calculated spectra for pure *hs*-Co^{II} (gray line) and *ls*-Co^{III} (black line) phases. Calculations are taken from ref 65.

in the excitation process remained to be clarified.[65] More recently, this technique provided definitive evidence of the valence tautomeric nature of the transition in a two-centered cobalt−dioxolene complex.[28]

Figure 5 shows room-temperature XAS Co L_3 edge spectra of compounds **1** and **3**, the temperature dependence of the normalized Co L_3 edge spectra of **2** (extended $L_{2,3}$ edge spectra are reported in Figure S8, Supporting Information), and the *hs*-Co^{II} and *ls*-Co^{III} theoretical spectra calculated for the parent complex with unfunctionalized dioxolene ligand using a ligand field multiplet (LFM) approach.[65,66] XAS analysis of compounds **1** and **3** confirms a temperature-independent charge distribution, *ls*-Co^{III} and *hs*-Co^{II}, respectively, insensitive to irradiation with the X-ray beam. On the other hand, the 300 K spectrum of **2** presents a superposition of signals belonging to the two redox isomeric forms. Upon isothermal irradiation with X-rays at 300 K, the system does not show any beam-induced irreversible change of electronic state (see Figure S9, Supporting Information), in contrast to what has been found in previous studies of different switchable metallo-organic species.[67,68] On cooling from 300 to 100 K the main feature at 781.5 eV, associated with the *ls*-Co^{III} ion, gains intensity while the spectral band related to the *hs*-Co^{II} contribution flattens down. This indicates the occurrence of valence tautomeric interconversion, similar to what previously found for similar Co-based molecular switchable materials.[59,62,64,65] When lowering temperature from 100 to 10 K, XAS indicates an increase in $\gamma_{hs\text{-}Co(II)SQ}$ which is not observed by magnetometry. This strongly suggests that this is an X-ray-induced effect and can then be interpreted in terms of SOXIESST (soft X-ray-induced excited spin state), a reversible phenomenon previously observed for photoswitchable molecular systems.[65,69]

A quantitative estimate of the *hs*-Co^{II} thermal distribution profile is reported in Figure 6, as calculated from spectral

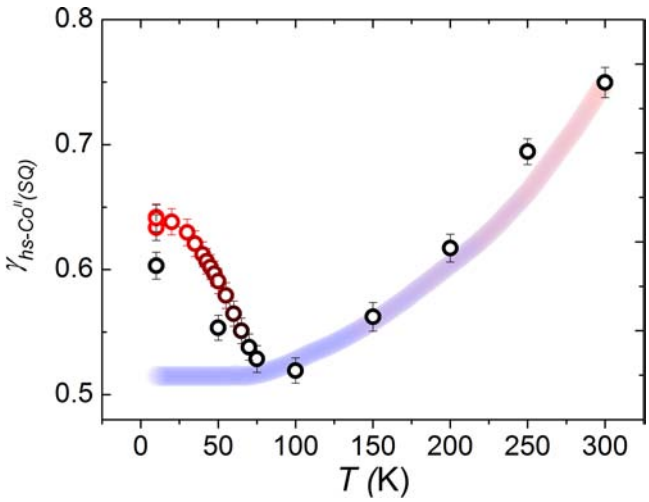

Figure 6. Thermal dependence of the *hs*-Co^{II} distribution profile obtained from deconvolution of X-ray absorption spectra (empty black circles), as described in the text. Empty circles, fading from red to black, display the thermally activated relaxation (measured at a 0.3 K/min warming rate) after 904 nm laser light irradiation, and colored band is the conversion profile obtained by rescaling magnetic measurements.

deconvolution using the theoretical spectra as limiting compositional references for the electronic states of **2**: it displays a smooth conversion profile in the 100−300 K range, in accordance with magnetometric analysis. The presence of a remaining fraction of $\gamma_{hs\text{-}Co(II)SQ}$ phase at low temperature is confirmed by this technique and estimated in 52% of the overall Co content to be compared with the 29% estimated with standard magnetometry. This apparent discrepancy can be explained by considering the different sample preparation conditions (slow crystallization vs drop cast) as well as detection techniques employed in the two cases. While magnetometry probes the total amount of the sample, XAS in total electron yield detection mode investigates only the few most external nanometers of the sample, where structural differences in the molecular surrounding, which affect the low-temperature charge distribution of the sample, may easily occur.[65]

Besides thermal- and X-ray-driven VT, XAS spectra allowed to point out the laser light-induced transition, evidencing an additional increase of the *hs*-Co^{II} feature when the sample was irradiated with a 904 nm laser light for 30 min at 10 K. The photoconverted *ls*-Co^{III} percentage increases from 11% found by magnetometry to 25% observed with XAS: such discrepancy must be related to the different detection modes of the two techniques, as discussed above, and to the non-innocent nature of the X-ray beam on the charge distribution of the sample. Finally, following the procedure carried out in the magnetometric case for determining T_{LIESST}, we monitored the temperature dependence of the photoinduced *hs*-Co^{II} molar fraction after laser irradiation with XAS (Figure S10, Supporting Information). Here, the T_{LIESST} value increases

dx.doi.org/10.1021/ic4011949 | *Inorg. Chem.* 2013, 52, 11798−11805

from 49 to 60 K: in this case, however, differences in the temperature control setup and noninnocence of X-rays on the low-temperature electronic configuration of **2** may play a role in determining the minimum in the first-derivative plot of the thermal distribution profile of the *hs*-Co^{II}(SQ) photoinduced molar fraction.

CONCLUSIONS

In this work we reported the synthesis and spectroscopic and magnetic characterization of a family of dinuclear cobalt−dioxolene complexes with a differently methylated tetradentate N-donating ancillary ligand, featuring a double thioetheric moiety as intramolecular link. To the best of our knowledge, this is the first report of functionalization of the coordination core with a thioether bridge in valence tautomeric molecular complexes. Temperature-dependent magnetometric analysis confirms that chemically driven tuning of the redox potential of the $[Co(Me_ntpa)]^{3+/2+}$ couple is possible in this molecular context as well: consequently, while **1** and **3** feature *ls*-Co^{III}(Cat) and *hs*-Co^{II}(SQ) temperature-independent charge distributions, respectively, **2** displays a partial entropy-driven switchability in the temperature range investigated. The time dependence of the magnetic signal of **2** under irradiation at 10 K with laser light matching the LMCT transition energy reveals a photoswitchable behavior with the energy barrier to relaxation only slightly lowered by chemical functionalization with the thioetheric moiety.

The robustness of the Co−diox switchable core toward functionalization with a thioetheric functional group affords a simple chemical means to use VT systems as building blocks for more complex chemical architectures as well as for surface functionalization purposes. In this regard, X-ray photoelectron spectroscopy was found to be a useful in-house technique for semiquantitative determination of the elemental composition and charge distribution of the different complexes in the solid state, allowing us to measure energy shifts and changes in the spectral patterns of the investigated family of complexes. XAS experiments, moreover, pointed out the stability of complexes **1**−**3** under X-ray flux, along with the possibility to safely monitor their temperature- and light-dependent electronic configurations. These findings constitute a preliminary step for analysis of the conversion behavior of Co−dioxolene switchable complexes in nanostructured environment like surface deposits, as requested for exploitation in working molecular devices.

ASSOCIATED CONTENT

Supporting Information

2D NOESY NMR spectrum of the diox-*S*-diox ligand, electronic, vibrational and XPS spectra of the **1**−**3** complexes, magnetic and XAS measurements of the decay kinetics of the photo-induced phase of **2**. This material is available free of charge via the Internet at http://pubs.acs.org.

AUTHOR INFORMATION

Corresponding Author

*Phone: +39 055 4573269. Fax: +39 055 4573372. E-mail: giordano.poneti@unifi.it

Notes

The authors declare no competing financial interest.

ACKNOWLEDGMENTS

We thank Dr. Julio Criginski Cezar and Dr. Nick Brookes for measurement of X-ray absorption spectra and the European Synchrotron Radiation Facility for the allocated beam time under Project HE-3523. We are grateful to Dr. Angelo Gallo (CERM, University of Florence) for helping in acquisition of the 2D NOESY NMR analysis and Dr. G. Giambastiani (ICCOM-CNR) for TGA measurements. Financial support from EC through the ERC Advanced Grant "MolNanoMAS" is gratefully acknowledged.

REFERENCES

(1) Gutlich, P.; Goodwin, H. A. *Spin Crossover in Transition Metal Compounds I*; Springer-Verlag: Berlin, Germany, 2004; Vol. *233*, p 1.
(2) Dei, A.; Gatteschi, D. *Angew. Chem., Int. Ed.* **2011**, *50*, 11852.
(3) Prins, F.; Monrabal-Capilla, M.; Osorio, E. A.; Coronado, E.; van der Zant, H. S. J. *Adv. Mater.* **2011**, *23*, 1545.
(4) Dei, A.; Gatteschi, D.; Sangregorio, C.; Sorace, L. *Acc. Chem. Res.* **2004**, *37*, 827.
(5) Hendrickson, D. N.; Pierpont, C. G. *Spin Crossover in Transition Metal Compounds II*; Springer-Verlag: Berlin, Germany, 2004; Vol. *234*, p 63.
(6) Day, M. B. R. a. P. *Adv. Inorg. Chem. Radiochem.* **1967**, *10*, 248.
(7) Beni, A.; Carbonera, C.; Dei, A.; Letard, J. F.; Righini, R.; Sangregorio, C.; Sorace, L. *J. Braz. Chem. Soc.* **2006**, *17*, 1522.
(8) Richardson, D. E.; Sharpe, P. *Inorg. Chem.* **1993**, *32*, 1809.
(9) Buchanan, R. M.; Pierpont, C. G. *J. Am. Chem. Soc.* **1980**, *102*, 4951.
(10) Jung, O.-S.; Jo, D. H.; Lee, Y.-A.; Conklin, B. J.; Pierpont, C. G. *Inorg. Chem.* **1997**, *36*, 19.
(11) Sato, O.; Cui, A.; Matsuda, R.; Tao, J.; Hayami, S. *Acc. Chem. Res.* **2007**, *40*, 361.
(12) Evangelio, E.; Ruiz-Molina, D. *Eur. J. Inorg. Chem.* **2005**, 2957.
(13) Dei, A.; Feis, A.; Poneti, G.; Sorace, L. *Inorg. Chim. Acta* **2008**, *361*, 3842.
(14) Roux, C.; Adams, D. M.; Itie, J. P.; Polian, A.; Hendrickson, D. N.; Verdaguer, M. *Inorg. Chem.* **1996**, *35*, 2846.
(15) Caneschi, A.; Dei, A.; de Biani, F. F.; Gutlich, P.; Ksenofontov, V.; Levchenko, G.; Hoefer, A.; Renz, F. *Chem.—Eur. J.* **2001**, *7*, 3926.
(16) Li, B.; Yang, F.-L.; Tao, J.; Sato, O.; Huang, R.-B.; Zheng, L.-S. *Chem. Commun.* **2008**, 6019.
(17) Markevtsev, I. N.; Monakhov, M. P.; Platonov, V. V.; Mischenko, A. S.; Zvezdin, A. K.; Bubnov, M. P.; Abakumov, G. A.; Cherkasov, V. K. *J. Magn. Magn. Mater.* **2006**, *300*, E407.
(18) Sato, O.; Tao, J.; Zhang, Y. Z. *Angew. Chem., Int. Ed.* **2007**, *46*, 2152.
(19) Balde, C.; Desplanches, C.; Guetlich, P.; Freysz, E.; Letard, J. F. *Inorg. Chim. Acta* **2008**, *361*, 3529.
(20) Dei, A.; Poneti, G.; Sorace, L. *Inorg. Chem.* **2010**, *49*, 3271.
(21) Gural'skiy, I. y. A.; Quintero, C. M.; Molnar, G.; Fritsky, I. O.; Salmon, L.; Bousseksou, A. *Chem.—Eur. J.* **2012**, *18*, 9946.
(22) Cavallini, M.; Bergenti, I.; Milita, S.; Ruani, G.; Salitros, I.; Qu, Z. R.; Chandrasekar, R.; Ruben, M. *Angew. Chem., Int. Ed.* **2008**, *47*, 8596.
(23) Miyamachi, T.; Gruber, M.; Davesne, V.; Bowen, M.; Boukari, S.; Joly, L.; Scheurer, F.; Rogez, G.; Yamada, T. K.; Ohresser, P.; Beaurepaire, E.; Wulfhekel, W. *Nat. Commun.* **2012**, *3*, 1.
(24) Warner, B.; Oberg, J. C.; Gill, T. G.; El Hallak, F.; Hirjibehedin, C. F.; Serri, M.; Heutz, S.; Arrio, M.-A.; Sainctavit, P.; Mannini, M.; Poneti, G.; Sessoli, R.; Rosa, P. *J. Phys. Chem. Lett.* **2013**, *4*, 1546.
(25) Droghetti, A.; Sanvito, S. *Phys. Rev. Lett.* **2011**, *107*, 047201.
(26) Beni, A.; Dei, A.; Laschi, S.; Rizzitano, M.; Sorace, L. *Chem.—Eur. J.* **2008**, *14*, 1804.
(27) Dapporto, P.; Dei, A.; Poneti, G.; Sorace, L. *Chem.—Eur. J.* **2008**, *14*, 10915.
(28) Alley, K. G.; Poneti, G.; Robinson, P. S. D.; Nafady, A.; Moubaraki, B.; Aitken, J. B.; Drew, S. C.; Ritchie, C.; Abrahams, B. F.;

Hocking, R. K.; Murray, K. S.; Bond, A. M.; Harris, H. H.; Sorace, L.; Boskovic, C. *J. Am. Chem. Soc.* **2013**, *135*, 8304.
(29) Letard, J. F. *J. Mater. Chem.* **2006**, *16*, 2550.
(30) Shul'ga, Y. M.; Bulatov, A. V.; Gould, R. A. T.; Konze, W. V.; Pignolet, L. H. *Inorg. Chem.* **1992**, *31*, 4704.
(31) Wagner, C. D.; Davis, L. E.; Zeller, M. V.; Taylor, J. A.; Raymond, R. H.; Gale, L. H. *Surf. Interface Anal.* **1981**, *3*, 211.
(32) Finley, K. T. In *Quinonoid Compounds*; Patai, S., Ed.; John Wiley and Sons, Ltd.: Chichester, UK, Vol. 2.
(33) Yadav, J. S.; Swamy, T.; Reddy, B. V. S.; Rao, D. K. *J. Mol. Catal. A: Chem.* **2007**, *274*, 116.
(34) Aviram, A.; Roland, P. In *Molecular Electronics: Science and Technology*; Aviram, A., Ratner, M., Eds.; New York Academy of Sciences: New York, 1998; Vol. *852*, p 339.
(35) Arumugam, S.; Popik, V. V. *J. Am. Chem. Soc.* **2012**, *134*, 8408.
(36) Kahn, O. *Molecular magnetism*; VCH: New York, 1993.
(37) Bencini, A.; Beni, A.; Costantino, F.; Dei, A.; Gatteschi, D.; Sorace, L. *Dalton Trans.* **2006**, 722.
(38) Alley, K. G.; Poneti, G.; Aitken, J. B.; Hocking, R. K.; Moubaraki, B.; Murray, K. S.; Abrahams, B. F.; Harris, H. H.; Sorace, L.; Boskovic, C. *Inorg. Chem.* **2012**, *51*, 3944.
(39) An increase of the $\chi_M T$ product of **2** to 5.21 emu·K/mol is observed when heating up **2** to 380 K, in analogy to what was previously found in similar systems.[37] We attribute this behavior to the combined effect of VT transition and partial loss of crystallization solvent, revealed by thermogravimetric analysis (Figure S4, Supporting Information), even if in principle partial damaging of the sample may occur at the highest temperature. After this thermal treatment, however, **2** kept on displaying a reversible VT transition.
(40) Hearns, N. G. R.; Korčok, J. L.; Paquette, M. M.; Preuss, K. E. *Inorg. Chem.* **2006**, *45*, 8817.
(41) Tayagaki, T.; Galet, A.; Molnar, G.; Munoz, M. C.; Zwick, A.; Tanaka, K.; Real, J. A.; Bousseksou, A. *J. Phys. Chem. B* **2005**, *109*, 14859.
(42) Chamberlin, R. V.; Mozurkewich, G.; Orbach, R. *Phys. Rev. Lett.* **1984**, *53*, 1025.
(43) Letard, J. F.; Capes, L.; Chastanet, G.; Moliner, N.; Letard, S.; Real, J. A.; Kahn, O. *Chem. Phys. Lett.* **1999**, *313*, 115.
(44) Carbonera, C.; Dei, A.; Letard, J. F.; Sangregorio, C.; Sorace, L. *Angew. Chem., Int. Ed.* **2004**, *43*, 3136.
(45) Ohno, Y. *J. Electron Spectrosc. Relat. Phenom.* **2008**, *165*, 1.
(46) Mazalov, L. N.; Asanov, I. P.; Varnek, V. A. *J. Electron Spectrosc. Relat. Phenom.* **1998**, *96*, 209.
(47) Koziel, M.; Podgajny, R.; Kania, R.; Lebris, R.; Mathoniere, C.; Lewinski, K.; Kruczala, K.; Rams, M.; Labrugere, C.; Bousseksou, A.; Sieklucka, B. *Inorg. Chem.* **2010**, *49*, 2765.
(48) Mathoniere, C.; Podgajny, R.; Guionneau, P.; Labrugere, C.; Sieklucka, B. *Chem. Mater.* **2005**, *17*, 442.
(49) Tokoro, H.; Ohkoshi, S.; Matsuda, T.; Hashimoto, K. *Inorg. Chem.* **2004**, *43*, 5231.
(50) Vertelman, E. J. M.; Maccallini, E.; Gournis, D.; Rudolf, P.; Bakas, T.; Luzon, J.; Broer, R.; Pugzlys, A.; Lummen, T. T. A.; van Loosdrecht, P. H. M.; van Koningsbruggen, P. *J. Chem. Mater.* **2006**, *18*, 1951.
(51) Ohtsu, H.; Tanaka, K. *Chem.—Eur. J.* **2005**, *11*, 3420.
(52) Joly, V. L. J.; Joy, P. A.; Date, S. K.; Gopinath, C. S. *Phys. Rev. B* **2002**, *65*, 184416.
(53) Ivanova, T.; Naumkin, A.; Sidorov, A.; Eremenko, I.; Kiskin, M. *J. Electron Spectrosc. Relat. Phenom.* **2007**, *156*, 200.
(54) Ivanova, T. M.; Shchukarev, A. V.; Linko, R. V.; Kiskin, M. A.; Sidorov, A. A.; Novotortsev, V. M.; Eremenko, I. L. *Russ. J. Inorg. Chem.* **2011**, *56*, 104.
(55) Lever, A. B. P. *Inorganic Electronic spectroscopy*; Elsevier: New York, 1986.
(56) Biesinger, M. C.; Payne, B. P.; Grosvenor, A. P.; Lau, L. W. M.; Gerson, A. R.; Smart, R. S. C. *Appl. Surf. Sci.* **2011**, *257*, 2717.
(57) Sessoli, R.; Mannini, M.; Pineider, F.; Cornia, A.; Sainctavit, Ph. In *Magnetism and Synchrotron Radiation: New Trends*; Beaurepaire, E., Bulou, H., Scheurer, F., Kappler, J. P., Eds.; Springer-Verlag: Berlin, Germany, 2010; Vol. *133*, p 279.
(58) Yokoyama, T.; Kiguchi, M.; Ohta, T.; Sato, O.; Einaga, Y.; Hashimoto, K. *Phys. Rev. B* **1999**, *60*, 9340.
(59) Briois, V.; Moulin, C. C. D.; Sainctavit, Ph.; Brouder, C.; Flank, A. M. *J. Am. Chem. Soc.* **1995**, *117*, 1019.
(60) Lee, J. J.; Sheu, H. S.; Lee, C. R.; Chen, J. M.; Lee, J. F.; Wang, C. C.; Huang, C. H.; Wang, Y. *J. Am. Chem. Soc.* **2000**, *122*, 5742.
(61) Gopakumar, T. G.; Matino, F.; Naggert, H.; Bannwarth, A.; Tuczek, F.; Berndt, R. *Angew. Chem., Int. Ed.* **2012**, *51*, 6262.
(62) Poneti, G.; Mannini, M.; Sorace, L.; Sainctavit, Ph.; Arrio, M.-A.; Rogalev, A.; Wilhelm, F.; Dei, A. *ChemPhysChem* **2009**, *10*, 2090.
(63) Bin-Salamon, S.; Brewer, S. H.; Depperman, E. C.; Franzen, S.; Kampf, J. W.; Kirk, M. L.; Kumar, R. K.; Lappi, S.; Peariso, K.; Preuss, K. E.; Shultz, D. A. *Inorg. Chem.* **2006**, *45*, 4461.
(64) Yokoyama, T.; Okamoto, K.; Nagai, K.; Ohta, T.; Hayami, S.; Gu, Z. Z.; Nakajima, R.; Sato, O. *Chem. Phys. Lett.* **2001**, *345*, 272.
(65) Poneti, G.; Mannini, M.; Sorace, L.; Sainctavit, Ph.; Arrio, M.-A.; Otero, E.; Cezar, J. C.; Dei, A. *Angew. Chem., Int. Ed.* **2010**, *49*, 1954.
(66) Thole, B. T.; Cowan, R. D.; Sawatzky, G. A.; Fink, J.; Fuggle, J. C. *Phys. Rev. B* **1985**, *31*, 6856.
(67) Collison, D.; Garner, C. D.; McGrath, C. M.; Mosselmans, J. F. W.; Pidcock, E.; Roper, M. D.; Searle, B. G.; Seddon, J. M. W.; Sinn, E.; Young, N. A. *J. Chem. Soc., Dalton Trans.* **1998**, 4179.
(68) Collison, D.; Garner, C. D.; McGrath, C. M.; Mosselmans, J. F. W.; Roper, M. D.; Seddon, J. M. W.; Sinn, E.; Young, N. A. *J. Chem. Soc., Dalton Trans.* **1997**, 4371.
(69) Arrio, M. A.; Long, J.; Moulin, C. C. D.; Bachschmidt, A.; Marvaud, V.; Rogalev, A.; Mathoniere, C.; Wilhelm, F.; Sainctavit, Ph. *J. Phys. Chem. C* **2010**, *114*, 593.